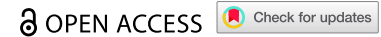



RESEARCH PAPER



## GdX inhibits the occurrence and progression of breast cancer by negatively modulating the activity of STAT3

Zhilin Chen<sup>a,b</sup>, Lu Xu<sup>c</sup>, Shibin Lin<sup>d</sup>, Hongjun Huang<sup>b</sup>, Qing Long<sup>b</sup>, and Jiwei Liu<sup>a</sup> 

<sup>a</sup>Department of Oncology, The First Affiliated Hospital of Dalian Medical University, Dalian, Liaoning, China; <sup>b</sup>Department of Breast Surgery, The First Affiliated Hospital of Hainan Medical University, Haikou, Hainan, China; <sup>c</sup>Department of Hematology, The First Affiliated Hospital of Hainan Medical University, Haikou, Hainan, China; <sup>d</sup>Department of Ultrasound, Hainan Women and Children's Medical Center, Haikou, Hainan, China

### ABSTRACT

**Aim:** To elucidate the biological functionality and regulatory mechanisms of GdX in breast cancer (BC). **Methods:** The examination of GdX expression in human BC tissues and cell lines was conducted through immunohistochemical (IHC) and Western blot. Cell proliferation capacity was assessed via the CCK-8 and colony formation assay, while cell migration was determined through the wound healing assay. The expression levels of BCL-XL, Cyclin D1, and C-myc gene were quantified using RT-qPCR and Western blot. In vivo tumor growth was evaluated in nude mice xenografted with MDA-MB-231 cells overexpressing GdX, and a mouse model with GdX-deficient BC was established to observe the impact of GdX on BC formation and metastasis. Dual-luciferase reporter assay and immunofluorescence were employed to confirm the interaction between GdX and STAT3. Western blot was employed to validate the influence of GdX overexpression on the phosphorylation process of STAT3. **Results:** GdX exhibited low expression in the cancer tissues of BC patients and cell lines. MDA-MB-231 and MCF-7 cells overexpressing GdX displayed a notable reduction in proliferation and diminished migratory capabilities, accompanied by downregulated mRNA and protein expression of BCL-XL, Cyclin D1, and C-myc. In the xenograft mouse model, heightened GdX expression correlated with a decelerated in vivo tumor growth. Furthermore, in mice deleting GdX, both the quantity and weight of tumors increased, along with evident pulmonary metastasis. Mechanistically, STAT3 emerged as a downstream target gene of GdX. **Conclusions:** GdX exerts its inhibitory effects on the initiation and progression of BC by negatively modulating the phosphorylation of STAT3.

### ARTICLE HISTORY

Received 20 June 2024  
Revised 16 October 2024  
Accepted 18 October 2024

### KEYWORDS

Breast cancer; GdX; signal transducer and activator of transcription 3; phosphorylation

### Introduction

Breast cancer (BC) stands as a prevalent malignant tumor that gravely jeopardizes the health of women, constituting a primary contributor to global female cancer-related fatalities.<sup>1</sup> This malignancy originates in the breast cells and has the potential to metastasize to other organs within the body.<sup>2,3</sup> Its clinical manifestations encompass palpable masses, pain, swelling, nipple discharge, or alterations in the shape and dimensions of the breast.<sup>4</sup> With the exacerbation of environmental pollution, particularly the proliferation of chemical products in daily life, the incidence of BC continues to escalate.<sup>5</sup> In the past decade, notable progress has been achieved in the diagnostic realm of BC. Nevertheless, the overall prognosis for BC remains sub-optimal due to the majority of patients receiving an initial diagnosis at an advanced stage, often accompanied by metastasis.<sup>6,7</sup> The complex biological process of BC proliferation and metastasis involves the activation or suppression of genes through epigenetic modifications.<sup>8</sup> The precise molecular mechanisms remain predominantly elusive. Consequently, the identification of potential biomarkers, serving as indicators for BC, has been pivotal in mitigating its incidence and augmenting the effectiveness of treatment.

GdX, situated as an X-linked gene in the G6PD cluster on the X chromosome (Xq28), is also recognized under the nomenclature Ubiquitin-like protein 4A (UBL4A), having been cloned by the Italian Daniela Toniolo research team in 1988.<sup>9</sup> GdX, recognized as a housekeeping gene encoding a petite protein featuring an N-terminal ubiquitin-like domain, does not exhibit any ubiquitin-related activity.<sup>10</sup> Nevertheless, GdX possesses a diverse array of functions and actively participates in various cellular events, encompassing ER-associated degradation, mediation of cell death induced by DNA damage, involvement in bone modeling, modulation of inflammatory and innate immune responses, cell migration, and engagement in anti-tumorigenesis, among others,<sup>11-19</sup> However, the biological functions of GdX in the regulation of signaling within the context of highly heterogeneous BC remain elusive.

The Signal Transducer and Activator of Transcription (STAT) family possesses the capability to integrate signals from cytokines and growth factors, thereby regulating the various cellular processes at the transcriptional level.<sup>20</sup> Among the seven members of the STAT family, STAT3, a pivotal component, exhibits sustained activation across all subtypes of BC. An escalating body of research underscores the

critical role played by activation of STAT3 in crucial processes in cells such as proliferation, apoptosis, angiogenesis, immune response, and metastasis in BC cells.<sup>21,22</sup> Prior studies have identified that GdX has the capacity to stimulate the specific dephosphorylation of STAT3, thereby inhibiting the STAT3 signaling pathway and consequently suppressing tumorigenesis as well as tumor development. Wang et al., employing GdX-deficient mice, induced sustained activation of STAT3, providing evidence that the absence of GdX could promote tumorigenesis and tumor development in colitis-associated colorectal cancer by enhancing the activity of STAT3.<sup>23</sup> Hence, we posit that GdX might exert its anti-BC effects by modulating the phosphorylation levels of STAT3.

In this investigation, the assessment of GdX expression was conducted in clinical BC samples and BC cell lines. Subsequently, we established BC cells overexpressing GdX through lentiviral transfection, xenografts in mice, as well as purchase transgenic mice for hybridization to construct GdX knockout mice model. The aim of our study is evaluating the biological function of GdX and delve into the underlying regulatory mechanisms of GdX both *in vivo* and *in vitro*.

## Material and methods

### Clinical sample

Cancer and paracancerous tissue specimens from 185 patients diagnosed with BC between 2010 and 2020 at Beijing 301 hospital and The First Affiliated Hospital of Hainan Medical College were collected. The clinical data of the patients, encompassing age, clinical stage, pathology, P53 and pSTAT3 level, among other parameters, were also obtained. The study adhered to the principles of the Declaration of Helsinki, with signed informed consent obtained from the patients or their family members. All experimental procedures received approval from the Medical Ethics Committee of The First Affiliated Hospital of Hainan Medical College (No. 2021082).

### Cell culture

The human normal breast epithelial cell line (MCF-10a) and human BC cell lines (MDA-MB-231, MCF-7, SKBR3, HCC1937 and MDA-MB-468) were procured from Procell Life Science & Technology Co., Ltd. (Wuhan, China). The cells were grown in RPMI-1640 medium containing 10% FBS, 100 mg/mL streptomycin, and 100 U/mL penicillin, keeping in a humidified incubator maintained with 5% CO<sub>2</sub> at 37°C. The medium underwent replacement every 3 days, and cells were harvested upon reaching the logarithmic growth phase.

### Animals

Ten female BALB/c nude mice (4–5 weeks old) were purchased from Sipeifu Biotechnology Co., Ltd. (Beijing, China). The MMTV-PyMT transgenic mice were obtained from Shanghai Model Organisms Center, Inc. (Shanghai, China), while the conventional GdX knockout mice were constructed and saved by our laboratory. The mice were housed in the specific pathogen-free (SPF) animal room under a 12-hour light/dark cycle,

room temperature maintained at 22 ± 2°C, humidity set at 50%-60%, and free access to food and drinking water. All experimental procedures were approved by the Ethics Committee of Hainan Medical College (No. HYLL-2021-265).

### Immunohistochemical (IHC)

IHC samples were derived from cancer and paracancerous tissues of BC patients. After fixation, embedding, and dehydration, the tumor specimens were sliced into 5 μm sections. Following blocking, the sections were incubated overnight at 4°C with a specific rabbit polyclonal antibody against GdX. After washing with PBS, the sections were incubated with a secondary antibody at room temperature for 20 minutes. DAB staining solution was employed for staining, and counterstaining was performed with hematoxylin. Finally, the sections were observed under a microscope (Olympus CX41, Olympus Company, Japan).

### Western blot

Protein samples were prepared from breast cells or tumor tissues using RIPA buffer (BioTeke, Beijing, China). Equal amount of total protein was separated using 10% sodium dodecyl sulfate-polyacrylamide gel electrophoresis (SDS-PAGE), followed by transferred onto polyvinylidene difluoride (PVDF) membranes for blotting. The membrane was blocked with 5% skimmed milk for 1 h at room temperature, and then incubated with primary antibodies against GdX (Proteintech, 1: 1000), Bcl-XL (Proteintech, 1: 1000), c-Myc (Proteintech, 1: 2000), Cyclin D1 (Proteintech, 1: 5000), STAT3 (Cell Signaling Technology, 1: 1000), phospho-STAT3 (p-STAT3) (Cell Signaling Technology, 1: 2000), and GAPDH (Cell Signaling Technology, 1: 1000) at 4°C overnight. Subsequently, the membrane was incubated with HRP-Goat anti-rabbit secondary antibodies (Abcam, 1:10000) at room temperature for 2 h. The visualization of protein bands was achieved through the chemiluminescence (ECL) substrate (Thermo Fisher), followed by quantitative analysis by Image J software.

### GdX overexpression

GdX overexpression was achieved through the transfection of cells with lentivirus. The complementary DNA (cDNA) of GdX was successfully cloned into lentivirus-based vectors (GeneChem, China) in accordance with the manufacturer's protocols. Subsequently, the empty vector or GdX-overexpressing (GdX-OE) lentivirus was employed for transfecting MDA-MB-231 and MCF-7 cells. Stable cell lines were selected using puromycin to ensure stable integration of the lentiviral construct. The efficiency of GdX overexpression was assessed through RT-qPCR and Western blot, confirming the successful establishment of GdX overexpression cell lines.

### Quantitative real-time polymerase chain reaction (qRT-pcr)

TRIzol reagent (Invitrogen, USA) was utilized to isolate total RNAs from OS cells lines, and the PrimeScript™ RT reagent

kit (TransGen Biotech, China) was applied to reverse-transcribe the RNAs into cDNA. Afterward, the qPCR was conducted using an ABI Stepone plus fluorescence quantitative PCR instrument. The analysis of the relevant mRNA expression levels was carried out using the  $2^{-\Delta\Delta Ct}$  method, and GAPDH functioned as the internal reference. The sequences of the primers were as follows: GdX: sense, 5'-TCAGCAAGGC AGTGTCAGAG-3'; antisense, 5'-GAGGATGAACC GGAACCCAG-3'; Bcl-XL: sense, 5'-CGAGCAGTC AGCCAGAATC-3'; antisense, 5'-ATTGATGGCA CTGGGGGTCT-3'; c-Myc: sense, 5'-TGAGCCCC TAGTGCTGCAT-3'; antisense, 5'-AGCCCCGACT CCGACC TCTT-3'; Cyclin D1: sense, 5'-GACACCAATCT CCTCA ACGAC-3'; antisense, 5'-CCTCTTCGC ACTTCTGCTC-3'; GAPDH: sense, 5'-AATGTGTCCG TCGTGGATCT-3'; antisense, 5'-CATCGAAGGT GGAAGAGTGG-3'. The thermal cycling conditions were set to 96°C for 5 minutes, followed by 40 cycles of 95°C for 30 seconds and 68°C for 20 seconds.

### Cell viability assay

Cells were seeded into 96-well plates at a density of 5000 cells per well and cultured for 24 hours. Subsequently, 10  $\mu$ l of CCK-8 solution (BBI Life Sciences) was added to each well and incubated for 1 hour at 37°C in darkness. Absorbance at 450 nm was measured utilizing a microplate reader (Multiskan MK3, Thermo Labsystems).

### Colony formation assay

MDA-MB-231 and MCF-7 cells were seeded in the culture plates at a density of  $1.5 \times 10^3$  cells per well and incubated at 37°C in a 5% CO<sub>2</sub> atmosphere for 1 week to allow colony formation. The plates were subsequently stained with crystal violet solution for 30 minutes.

### Wound healing assay

MDA-MB-231 and MCF-7 cells were cultured in 6-well plates until they reached 70–80% confluency. Subsequently, the tips of sterile pipette heads were gently used to create straight scratches. Samples were collected at 0 hours and 24 hours of co-culture to observe cell migration. Images were captured via an inverted microscope, and the width of the scratch before and after co-culture was measured for analysis using Image J software.

### Xenograft nude mice model

MDA-MB-231 cells transfected with empty vector or GdX-overexpressing lentivirus were subcutaneously injected into the mammary fat pads of each nude mice at a concentration of  $1 \times 10^7$  cells per mouse to establish the xenograft model ( $n = 5$ /group). Tumor size was measured every two days, and the tumor volume were calculated (Tumor volume =  $0.5 \times \text{length} \times \text{width}$ ).<sup>2</sup> Continuous measurements and records were maintained for both tumor volume and body weight. Upon euthanizing the mice on the 30th day, tumors were excise, weighed, photographed, and prepared for subsequent analyses.

### Generation of GdX knockout mice

GdX knockout mice were generated using CRISPR/Cas9-mediated genome engineering. The guide RNA (gRNA) was designed to target the GdX gene exons and was co-injected with Cas9 into fertilized eggs. By crossing candidate knockout founder mice and wild-type mice, homozygous GdX knockout (GdX<sup>-/-</sup>) progeny were successfully generated via brother-sister matings. Subsequently, female GdX<sup>-/-</sup> mice were bred with male MMTV-PyMT mice to produce homozygous PyMT GdX<sup>-/-</sup> offspring. Female PyMT GdX<sup>+/+</sup> littermate mice served as the control. Palpable tumors of both PyMT GdX<sup>-/-</sup> and PyMT GdX<sup>+/+</sup> mice were monitored weekly. After euthanasia, lung tissues of mice were harvested, photographed, and weighed.

### Dual-luciferase reporter assays

The wild-type (WT) or mutant (MUT) sequences of STAT3 3'UTR, containing the putative GdX binding sites, were inserted into the pmirGLO plasmid (Promega, USA) to construct STAT3-WT and STAT3-MUT, respectively. Subsequently, cells were transfected with GdX-NC or GdX-overexpressing lentivirus along with corresponding luciferase reporter vector for 48 hours. The luciferase activity was assessed utilizing the Dual-luciferase Reporter<sup>®</sup> Assay System.

### Immunofluorescence

MDA-MB-231 cells were collected, and fixed with 4% paraformaldehyde, and blocked using 5% BSA. Following this, the cells were subjected to treatment with primary antibodies at 4°C overnight. After three washes with PBS, the cells were subsequently incubated with the secondary antibody for 1 hour. Cellular imaging was performed through a fluorescence microscope to observe the co-localization of GdX and STAT3 within the cells.

### Statistical analysis

All data were expressed as the mean  $\pm$  standard deviation (SD). PRISM<sup>®</sup> GraphPad 8.0 software, Tukey's post-hoc tests, and one- or two-way analysis of variance (ANOVA) were conducted to analyze all data. Each sample was evaluated in a minimum of three experimental replicates, and  $p < .05$  was considered a significant level.

## Results

### Correlation of GdX expression in BC patients and cells

In order to elucidate the expression of GdX in BC, tumor and paracancerous tissues from 185 patients definitively diagnosed with BC at our institution were subjected to IHC staining. The results revealed that GdX was predominantly expressed in the paracancerous tissues, while exhibiting low expression in the tumor tissues (Figure 1a). Further validation through Western blot analysis demonstrated significantly lower protein expression levels of GdX in the BC cell lines MCF-7 and MDA-MB-123 compared



to the non-tumorigenic breast epithelial cell line MCF-10a ( $p < .001$ , Figure 1b). Based on the levels of GdX expression, we categorized the 185 BC patients into two groups. Survival analysis revealed a negative correlation between GdX expression and BC prognosis, where higher GdX expression was associated with longer disease-free survival (DFS) and overall survival (OS) for patients (Figure 1c-d). Moreover, a further correlation analysis was conducted between GdX expression levels in the 185 BC patients and various clinicopathological indicators. The results indicated that the expression level of GdX was primarily associated with the primary tumor size, estrogen receptor therapy, chemotherapy status, as well as the expression levels of P53 and pSTAT3 (Table 1).

### Validation of transfection efficiency of BC cells overexpressing GdX

Clinical tissue and cell samples consistently demonstrate an inverse correlation between the malignancy of tumors and the expression levels of GdX. To further investigate the impact of GdX on the malignant progression of BC cells, we constructed

GdX overexpression lentivirus and transfected them into MCF-7 and MDA-MB-231 cells with relatively lower levels of GdX expression. As depicted in Figure 2, the results from RT-qPCR and Western blot analyses confirm the successful construction of BC cell lines MCF-7 and MDA-MB-231 with GdX overexpression.

### The influence of GdX levels on the malignant progression of BC

*In vitro*, the impact of GdX on the proliferative capacity of MDA-MB-231 and MCF-7 cells was assessed through CCK-8 assay (Figure 3a) and colony formation assay (Figure 3b). The results revealed a significant inhibition in the proliferation of MDA-MB-231 and MCF-7 cells upon GdX overexpression. Additionally, wound healing assay demonstrated that GdX overexpression markedly inhibited the migration of MDA-MB-231 and MCF-7 cells (Figure 3c). Furthermore, the expression levels of anti-apoptotic gene BCL-XL, cell cycle proteins Cyclin D1, and C-myc gene were evaluated through RT-qPCR (Figure 3d-e) and Western blot experiments (Figure 3f-g). The findings indicated a markedly inhibition in both mRNA

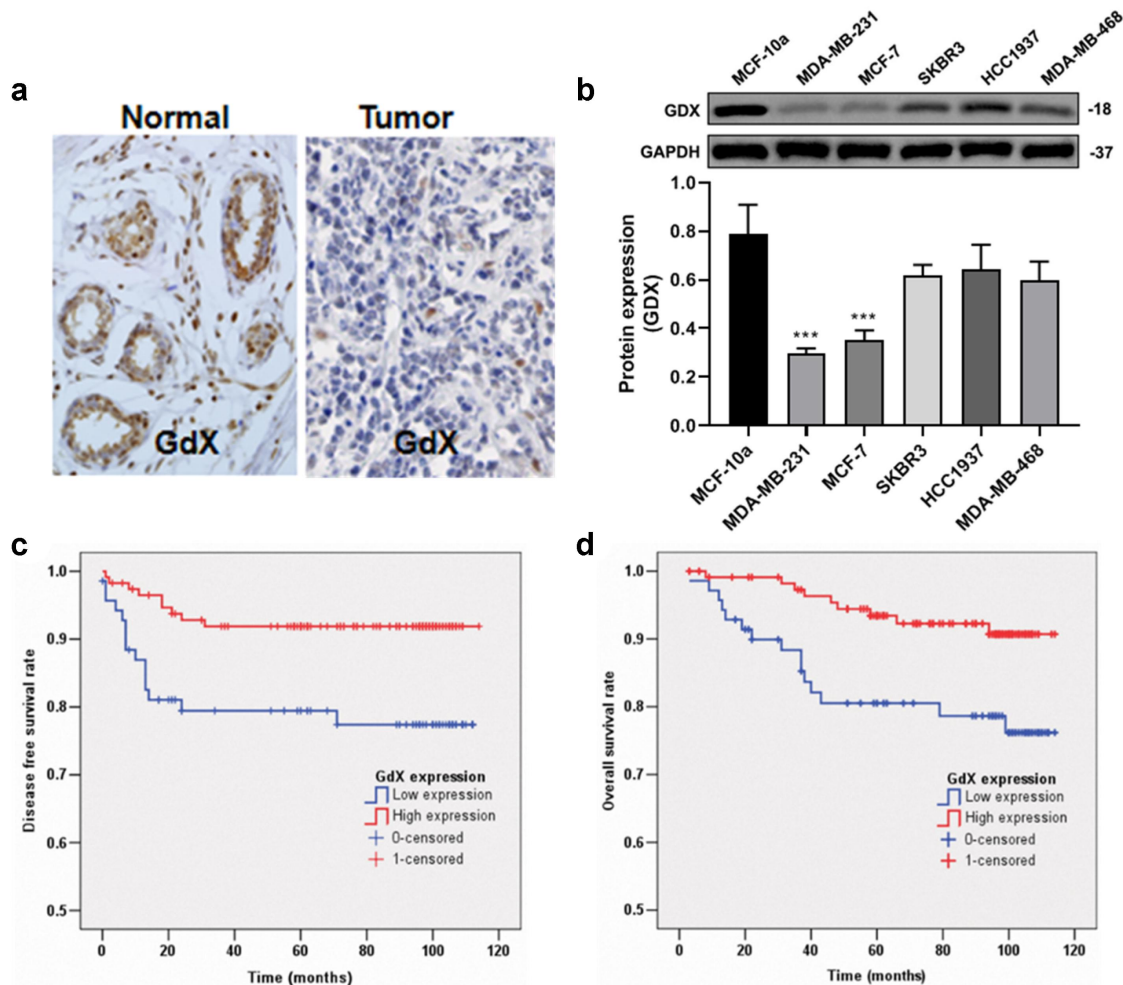


**Figure 1.** Correlation of GdX expression in breast cancer patients and cells. (a) Immunohistochemical staining was employed to analyze the expression of GdX in both breast cancer and adjacent normal tissues. (b) Western blot assays were conducted to assess the protein levels of GdX in the human normal breast epithelial cell line (MCF-10a) and human breast cancer cell lines (MDA-MB-231, MCF-7, SKBR3, HCC1937 and MDA-MB-468). \*\*\*,  $p < .001$ , vs. MCF-10a. (c) The disease-free survival rate and (d) overall survival rate was analyzed in the breast cancer patients with GdX high expression ( $n = 115$ ) and low expression ( $n = 70$ ).

**Table 1.** Relationship between gdx expression and clinicopathologic factors in 185 patients with breast cancer.

| Clinicopathological features | Category  | Total number (n = 185) | GdX expression |              | P Value  |
|------------------------------|-----------|------------------------|----------------|--------------|----------|
|                              |           |                        | High (n = 115) | Low (n = 70) |          |
| Age                          |           |                        | 54 ± 11.7      | 51.1 ± 11.8  | 0.1049   |
| T grade: tumor size          | ≥T2       | 106                    | 56 (52.8%)     | 50 (47.2%)   | 0.0022** |
|                              | ≤T1       | 79                     | 59 (74.7%)     | 20 (25.3%)   |          |
| Lymphatic invasion           | Negative  | 120                    | 78 (65.0%)     | 42 (35.0%)   | 0.2811   |
|                              | Positive  | 65                     | 37 (56.9%)     | 28 (43.1%)   |          |
| Stage                        | ≥IIB      | 54                     | 29 (53.7%)     | 25 (46.3%)   | 0.1302   |
|                              | ≤IIA      | 131                    | 86 (65.6%)     | 45 (34.4%)   |          |
| Pathology                    | DCIS      | 13                     | 9 (69.2%)      | 4 (30.8%)    | 0.7298   |
|                              | IDC/NOS   | 162                    | 99 (61.1%)     | 63 (38.9%)   |          |
|                              | Others    | 10                     | 7 (70.0%)      | 3 (30.0%)    |          |
| Menopause                    | MP-       | 82                     | 50 (61.0%)     | 32 (39.0%)   | 0.7666   |
|                              | MP+       | 103                    | 65 (63.1%)     | 38 (36.9%)   |          |
| Anti-Estrogen therapy        | None      | 58                     | 26 (44.8%)     | 32 (55.2%)   | 0.0011** |
|                              | Performed | 127                    | 89 (70.1%)     | 38 (29.9%)   |          |
| Chemotherapy                 | None      | 89                     | 66 (74.2%)     | 23 (25.8%)   | 0.0011** |
|                              | Performed | 96                     | 49 (51.0%)     | 47 (49.0%)   |          |
| Radiation                    | None      | 64                     | 39 (60.9%)     | 25 (39.1%)   | 0.8029   |
|                              | Performed | 121                    | 76 (62.8%)     | 45 (37.2%)   |          |
| ER                           | Negative  | 92                     | 52 (56.5%)     | 40 (43.4%)   | 0.1152   |
|                              | Positive  | 93                     | 63 (67.7%)     | 30 (32.3%)   |          |
| P53                          | Abnormal  | 52                     | 24 (46.2%)     | 28 (53.8%)   | 0.0054** |
|                              | Normal    | 133                    | 91 (68.4%)     | 42 (31.6%)   |          |
| pSTAT3                       | Negative  | 124                    | 85 (68.5%)     | 39 (31.5%)   | 0.0112*  |
|                              | Positive  | 61                     | 30 (49.2%)     | 31 (50.8%)   |          |

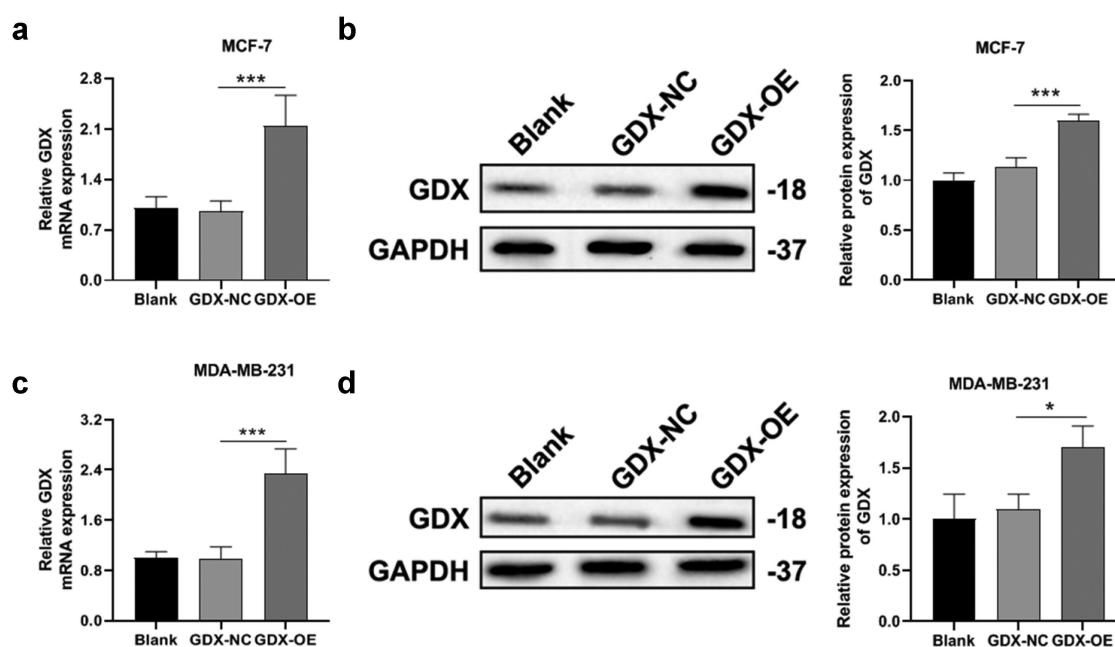


**Figure 2.** Validation of transfection efficiency of breast cancer cells overexpressing GdX. (a) RT-qPCR and (b) Western blot analyses were employed to assess the transfection efficiency of GdX in MCF-7 cells. (c) RT-qPCR and (d) Western blot analyses were conducted to evaluate the transfection efficiency of GdX in MDA-MB-231 cells. \*,  $p < .05$ , \*\*\*,  $p < .001$ , vs. GdX-nc.

and protein expression of these three factors upon GdX overexpression, underscoring the role of GdX overexpression in impeding the malignant progression of BC cells.

A nude mouse xenograft model was established to validate the impact of GdX on *in vivo* BC growth. As depicted in Figures 4a–c, the tumor volume and weight were significantly reduced in the GdX-OE group compared to the GdX-NC group. Tumor tissues of mice from both groups were collected, and GdX expression was assessed through RT-qPCR. The results revealed a substantial increase in GdX mRNA expression in the GdX-OE group compared to the GdX-NC group ( $p$

$< .001$ , Figure 4d), confirming the successful construction of the mouse model with GdX overexpression. Consistently, the expression levels of the anti-apoptotic gene BCL-XL, cell cycle proteins Cyclin D1, and C-myc gene were in line with the *in vitro* findings (Figure 4e–f).

Afterward, we aimed to observe the effect of GdX on BC formation and metastasis by constructing a mouse model with GdX deficiency. Female mice with specific knockout of GdX that have been constructed in our laboratory were mated with transgenic male MMTV-PyMT mice to obtain homozygous PyMT GdX<sup>-/-</sup> mice (Figure 5a). Furthermore, PyMT GdX<sup>-/-</sup>

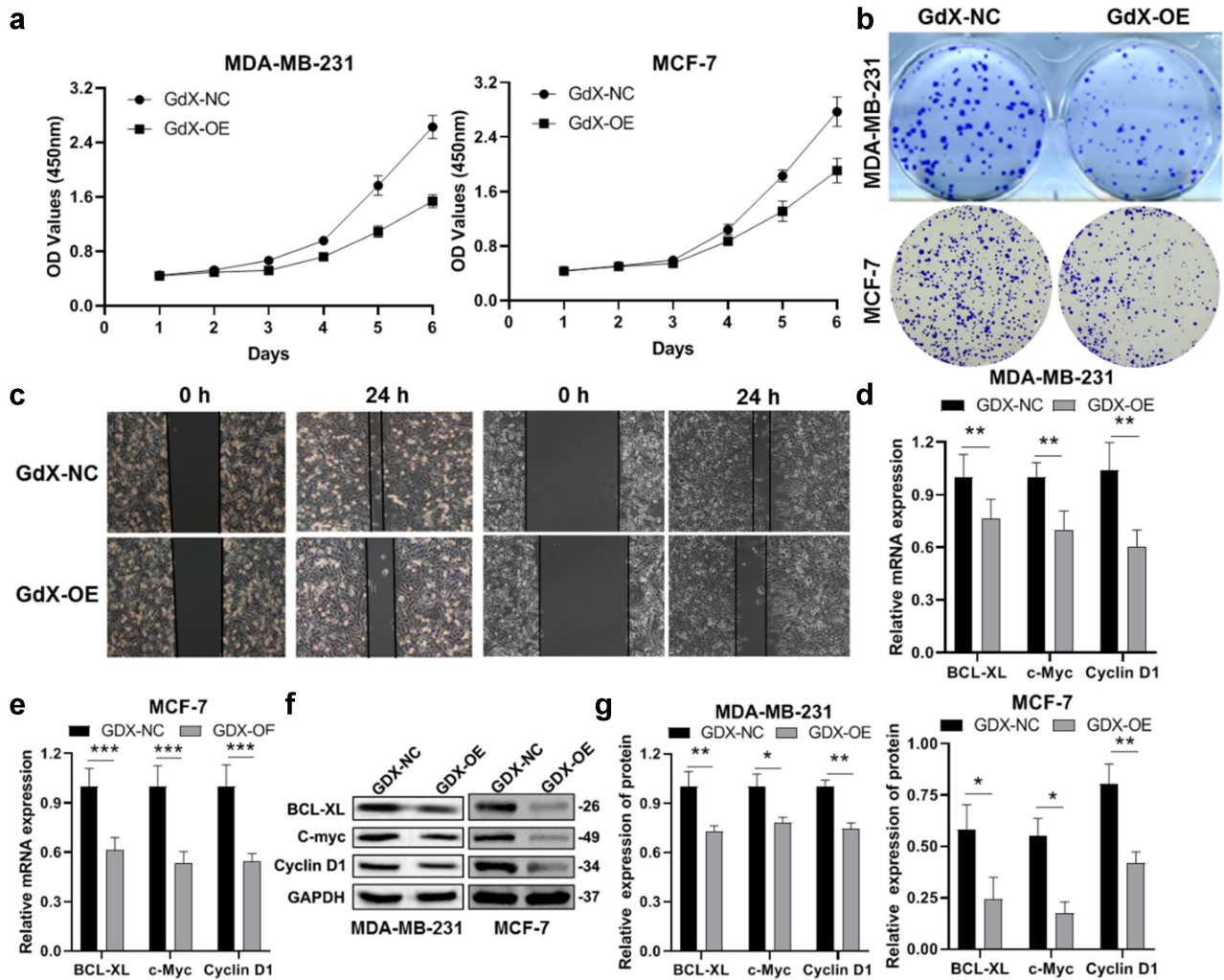


**Figure 3.** The impact of GdX overexpression on the malignant progression of MDA-MB-231 and MCF-7 cells was assessed *in vitro*. (a) CCK-8 assay and (b) colony formation assay were conducted to examine the influence of GdX overexpression on the proliferative capacity of MDA-MB-231 and MCF-7 cells. (c) Wound healing assay was employed to evaluate the effect of GdX overexpression on the migratory ability of MDA-MB-231 and MCF-7 cells. (d–e) rt-qPCR and (f–g) Western blot analyses were performed to measure the expression levels of the anti-apoptotic gene BCL-XL, cell cycle protein cyclin D1 and C-myc in MDA-MB-231 and MCF-7 cells overexpressing GdX. \*,  $p < .05$ , \*\*,  $p < .01$ , vs. GdX-nc.

mice exhibited an increased number and weight of tumors compared to PyMT GdX1<sup>+/+</sup> littermate mice (Figure 5b), along with evident pulmonary metastasis (Figure 5c).

### GdX specifically interacts with STAT3

The effect on STAT3 transcription under GdX overexpression or normal conditions was examined by dual luciferase assay, revealing that STAT3 serves as a downstream target gene of GdX (Figure 6a). Furthermore, for a more intuitive understanding of the expression distribution and the specific site of the two interacting proteins within the cells, immunofluorescence staining experiments were conducted. The results illustrated a clear co-localization of GdX and p-STAT3 in the cell nucleus, further indicating their interaction (Figure 6b). Subsequently, *in vivo* Western blot experiments were conducted to verify the effect of GdX overexpression on the phosphorylation process of STAT3. The results indicated that GdX overexpression significantly reduced STAT3 phosphorylation ( $p < .01$ , Figure 6c).

### Discussion

BC emerges as a global health concern, impacting women worldwide and leading to severe morbidity and mortality.<sup>24</sup> Tumor progression involves multiple factors, including cell proliferation, migration, cell cycle regulation, and metastasis. Existing literature indicates that GdX suppresses proliferation and metastasis in pancreatic ductal adenocarcinoma,<sup>25</sup> and overexpression of GdX has been shown to cause tumor regression in B16 cells.<sup>23</sup> In this study, we found that GdX expression was downregulated in BC patients and cell lines and was associated with poor DFS and OS. Both *in vitro* cell experiments and *in vivo* xenograft models demonstrated that GdX overexpression significantly inhibits BC progression. Conversely, GdX deficiency in mice resulted in increased tumor quantity and weight, along with notable pulmonary metastases. Mechanistically, GdX negatively regulates the STAT3 pathway, with overexpression leading to reduced STAT3 phosphorylation. This study suggests that targeting the GdX-STAT3 axis could be a promising therapeutic strategy for BC treatment.

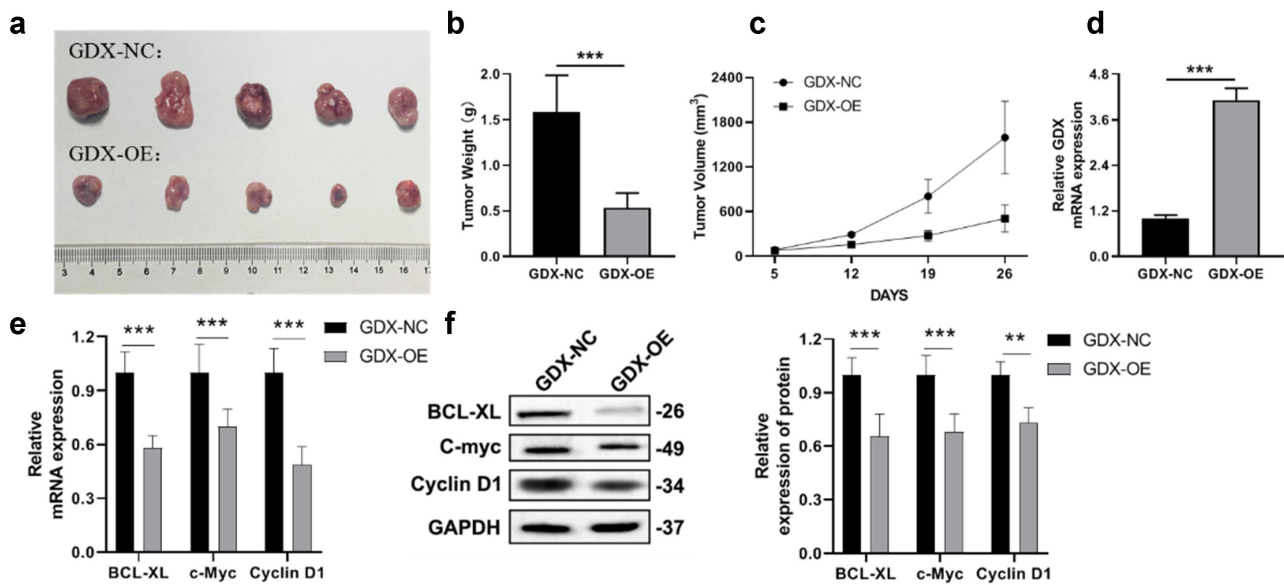


**Figure 4.** The impact of GdX overexpression on the malignant progression of breast cancer *in vivo*. (a) Gross images of the tumors. (b) Tumor weight. (c) Tumor volume. (d) RT-qPCR was employed to detect the mRNA expression of GdX in the tumors. (e) RT-qPCR and (f) Western blot analyses were performed to measure the expression levels of the anti-apoptotic gene BCL-XL, cell cycle protein cyclin D1 and C-myc in tumor tissues. \*\*,  $p < .01$ , \*\*\*,  $p < .001$ , vs. Gdx-nc.

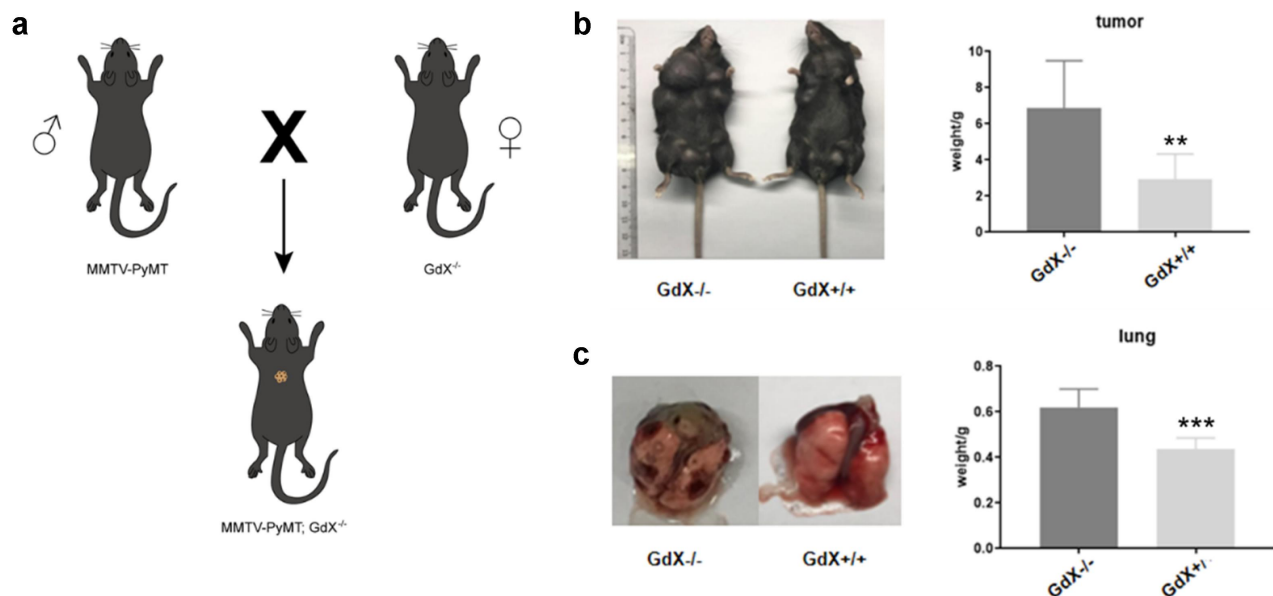


**Figure 5.** Effect of GdX deficiency on breast cancer formation and metastasis. (a) Schematic representation showing the generation of MMTV-PyMT mice with conventional GdX knockout. (b) The quantity and weight of tumors in mice; (c) pulmonary metastasis. \*\*,  $p < .01$ , \*\*\*,  $p < .001$ , vs. GdX<sup>-/-</sup>.

GdX, a single-copy gene conserved across evolution, is located on Xq28 and comprises 157 amino acids. Previous research indicates that GdX functions as a companion protein, facilitating the transport and processing of newly synthesized polypeptides within the endoplasmic reticulum.<sup>26</sup> It also plays a role in regulating migration, innate immune responses,<sup>14</sup> and DNA-damage-induced cell death.<sup>13</sup> In our study, we observed that GdX was downregulated in BC tissues and cell lines, correlating with poor prognosis, suggesting that GdX could serve as a potential prognostic biomarker for BC. This is consistent with findings from Chen et al.,<sup>11</sup> who analyzed UBL4A expression in PDAC patients and found that lower UBL4A protein levels were associated with worse outcomes.

The overexpression of GdX holds significant clinical potential for BC treatment, although further research is needed to fully elucidate its biological functions and mechanisms in BC. In our functional experiments, overexpression of GdX inhibited the progression of BC, the expression of several pro-growth genes crucial for tumor cell proliferation and survival, including Bcl-XL, Cyclin D1, and C-myc,<sup>27-29</sup> were examined in MDA-MB-231 and MCF-7 cells transfected with GdX, revealing an inhibitory effect on their expression, aligning with consistent outcomes in *in vivo* experiments. Furthermore, the mortality of BC patients is predominantly attributed to metastasis,<sup>3,30</sup> and our GdX-deficient mouse model showed increased tumor growth and pulmonary metastasis, further



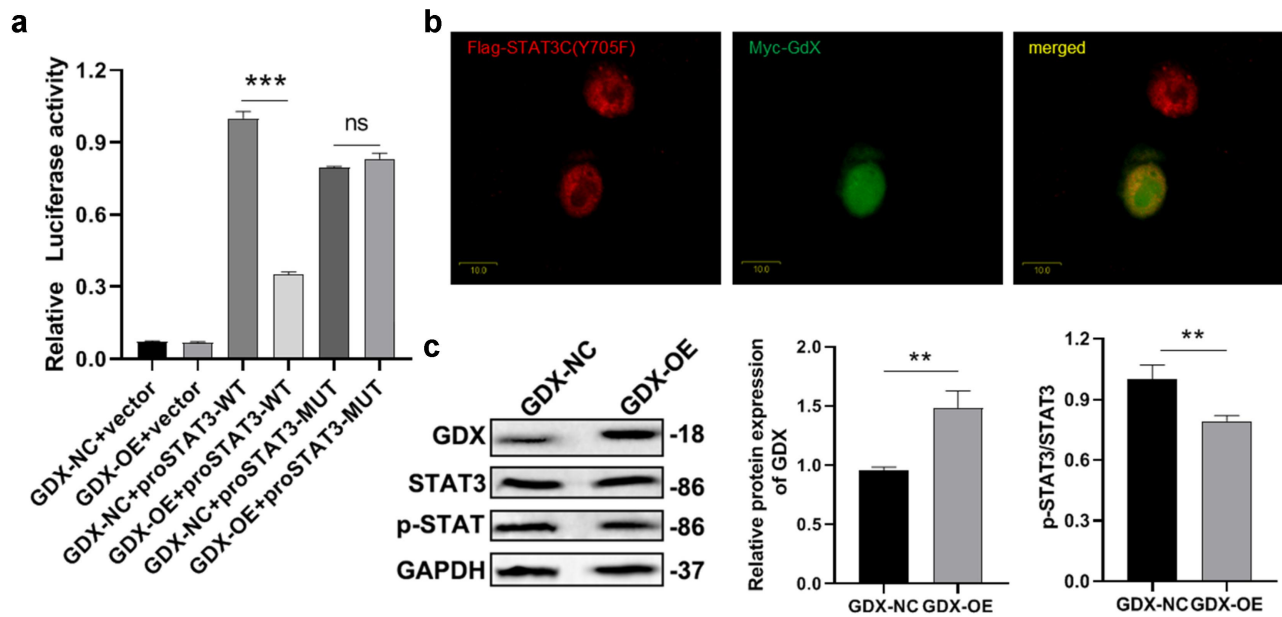


**Figure 6.** GdX specifically interacts with STAT3. (a) Dual luciferase assay results indicate that STAT3 is a downstream target gene of GdX; (b) immunofluorescence staining reveals the colocalization of GdX and p-STAT3 in the cell nucleus; (c) Western blot analysis assesses the impact of GdX overexpression on the phosphorylation levels of STAT3. \*,  $p < .05$ , \*\*,  $p < .01$ , \*\*\*,  $p < .001$ , vs. GdX-nc.

highlighting the critical role of GdX in BC progression and its potential as a prognostic biomarker and therapeutic target for drug development.

It is noteworthy that the anti-apoptotic gene BCL-XL, the cell cycle protein Cyclin D1 and C-myc are all downstream target genes of the cancer-associated gene STAT3,<sup>31</sup> which prompts our speculation that GdX might exert its anti-BC effects by modulating STAT3 activity. The activation of STAT3 holds crucial significance for the rapid proliferation of tumor cells, as it actively participates in both cell proliferation and survival. Corresponding to its role in cell proliferation, the STAT3 signaling pathway also has the capability to suppress apoptosis in cancer cells.<sup>32,33</sup> Earlier studies have documented that GdX inhibits tumorigenesis by inducing the dephosphorylation of STAT3.<sup>23</sup> In our study, STAT3 has been confirmed as a downstream target gene of GdX, with a conspicuous colocalization of GdX and phosphorylated STAT3 (p-STAT3) observed within the cell nucleus. Moreover, *in vivo* Western blot experiments have substantiated that the overexpression of GdX significantly diminishes the phosphorylation of STAT3. These findings collectively imply that GdX operates as a tumor suppressor by regulating the phosphorylation status of STAT3. Previous studies have shown that GdX promotes STAT3 dephosphorylation by mediating the interaction between TC45 (the nuclear isoform of TC-PTP) and STAT3.<sup>23</sup> Additionally, GdX is involved in inflammation-related tumorigenesis through the regulation of p-STAT3, and its role in inflammatory signaling pathways, such as NF- $\kappa$ B signaling, has been well established in inflammatory diseases.<sup>15</sup> However, the specific molecular mechanisms underlying the interaction between GdX and STAT3, as well as the signaling pathways involved, warrant further investigation. Moreover, exploring the potential links between GdX and other breast cancer-related genes

or signaling pathways, such as Src and JAK activation in STAT3-related breast cancer cells,<sup>23</sup> may provide new research perspectives and therapeutic targets to improve the prognosis of BC patients.

## Conclusions

Collectively, our findings reveal a significant downregulation of GdX expression in BC tumor samples and human BC cell lines, correlating negatively with a poor prognosis. Our study has elucidated the pivotal role of GdX in inhibiting the proliferation and migration of BC cells by suppressing the phosphorylation of STAT3. Furthermore, *in vivo* experiments, involving both GdX overexpression and knockout, have validated its influence on the malignant progression of BC and pulmonary metastasis. The outcomes of our research provide valuable insights for prognostic prediction, personalized therapy guidance, and the exploration of novel targeted treatment strategies in the context of BC.

## Disclosure statement

No potential conflict of interest was reported by the author(s).

## Funding

The present study was supported by Natural Science Foundation of Hainan Province [grant no. 822MS177].

## ORCID

Jiwei Liu  <http://orcid.org/0009-0005-5630-7989>



## Authors' contributions

Conceptualization ideas, Zhilin Chen; validation verification, Zhilin Chen, Lu Xu, and Shibin Lin; formal analysis, Lu Xu and Shibin Lin; investigation, Hongjun Huang and Qing Long; data curation, Hongjun Huang and Qing Long; writing – original draft preparation, Zhilin Chen; writing – review & editing, Jiwei Liu; visualization preparation, Jiwei Liu; funding acquisition, Zhilin Chen. All authors have read and agreed to the published version of the manuscript.

## Data availability statement

Data will be made available from corresponding author upon reasonable request.

## Ethics approval and consent to participate

All animal experiments were approved by the Medical Ethics Committee of The First Affiliated Hospital of Hainan Medical College (No. 2021082) and Ethics Committee of Hainan Medical College (No. HYLL-2021-265), and followed the National Research Council's Guide for the Care and Use of Laboratory Animals (1985); The euthanasia method in this study was informed by the American Veterinary Medical Association (AVMA) Guidelines for the Euthanasia of Animals (2020).

## References

- Bray F, Laversanne M, Sung H, Ferlay J, Siegel RL, Soerjomataram I, Jemal A. Global cancer statistics 2022: GLOBOCAN estimates of incidence and mortality worldwide for 36 cancers in 185 countries. *CA Cancer J Clin.* 2024;74(3):229–263. doi:10.3322/caac.21834.
- Thakur C, Qiu Y, Pawar A, Chen F. Epigenetic regulation of breast cancer metastasis. *Cancer Metastasis Rev.* 2024;43(2):597–619. doi:10.1007/s10555-023-10146-7.
- Wu S, Lu J, Zhu H, Wu F, Mo Y, Xie L, Song C, Liu L, Xie X, Li Y, et al. A novel axis of circKIF4A-miR-637-STAT3 promotes brain metastasis in triple-negative breast cancer. *Cancer Lett.* 2024;581:216508. doi:10.1016/j.canlet.2023.216508.
- Łukaszewicz S, Czeczulewski M, Forma A, Baj J, Sitarz R, Stanisławek A. Breast cancer—epidemiology, risk factors, classification, prognostic markers, and current treatment strategies—an updated review. *Cancers.* 2021;13(17):4287. doi:10.3390/cancers13174287.
- Wen X, Hou Y, Zhou L, Fang X. LINC00969 inhibits proliferation with metastasis of breast cancer by regulating phosphorylation of PI3K/AKT and ILP2 expression through HOXD8. *PeerJ.* 2023;11:e16679. doi:10.7717/peerj.16679.
- Li X, Jin F, Li Y. A novel autophagy-related lncRNA prognostic risk model for breast cancer. *J Cellular And Mol Med.* 2021;25(1):4–14. doi:10.1111/jcmm.15980.
- Wilcken NR. The importance of early breast cancer treatment: delay can be deadly. *The Med J Aust.* 2023;219(9):408–. doi:10.5694/mja2.52123.
- Barzaman K, Karami J, Zarei Z, Hosseinzadeh A, Kazemi MH, Moradi-Kalbolandi S, Safari E, Farahmand L. Breast cancer: biology, biomarkers, and treatments. *Int Immunopharmacol.* 2020;84:106535. doi:10.1016/j.intimp.2020.106535.
- Toniolo D, Persico M, Alcalay M. A “housekeeping” gene on the X chromosome encodes a protein similar to ubiquitin. *Proc Natl Acad Sci USA.* 1988;85(3):851–855. doi:10.1073/pnas.85.3.851.
- Peng SJ, Yao RR, Yu SS, Chen HY, Pang X, Zhang Y, Zhang J. UBL4A augments innate immunity by promoting the K63-linked ubiquitination of TRAF6. *J Immunol.* 2019;203(7):1943–1951. doi:10.4049/jimmunol.1800750.
- Chen H, Li L, Hu J, Zhao Z, Ji L, Cheng C, Zhang G, Zhang T, Li Y, Chen H, et al. UBL4A inhibits autophagy-mediated proliferation and metastasis of pancreatic ductal adenocarcinoma via targeting LAMP1. *J Exp & Clin Cancer Res.* 2019;38(1):1–18. doi:10.1186/s13046-019-1278-9.
- Xu Y, Cai M, Yang Y, Huang L, Ye Y. SGTA recognizes a noncanonical ubiquitin-like domain in the Bag6-Ubl4A-Trc35 complex to promote endoplasmic reticulum-associated degradation. *Cell Rep.* 2012;2(6):1633–1644. doi:10.1016/j.celrep.2012.11.010.
- Krenciute G, Liu S, Yucer N, Shi Y, Ortiz P, Liu Q, Kim B-J, Odejimi AO, Leng M, Qin J, et al. Nuclear BAG6-UBL4A-GET4 complex mediates DNA damage signaling and cell death. *J Biol Chem.* 2013;288(28):20547–20557. doi:10.1074/jbc.M112.443416.
- Zhao Y, Zhang H, Affonso C, Bonomo R, Mañas A, Xiang J. Deficiency in ubiquitin-like protein Ubl4A impairs migration of fibroblasts and macrophages. *Biochem Biophys Res Commun.* 2017;483(1):617–623. doi:10.1016/j.bbrc.2016.12.094.
- Liu C, Zhou Y, Li M, Wang Y, Yang L, Yang S, Feng Y, Wang Y, Wang Y, Ren F, et al. Absence of GdX/UBL4A protects against inflammatory diseases by regulating nf-kb signaling in macrophages and dendritic cells. *Theranostics.* 2019;9(5):1369. doi:10.7150/thno.32451.
- Peng S-J, Yao R-R, Yu S-S, Chen H-Y, Pang X, Zhang Y, Zhang J. UBL4A augments innate immunity by promoting the K63-linked ubiquitination of TRAF6. *The J Immunol.* 2019;203(7):1943–1951. doi:10.4049/jimmunol.1800750.
- Fu Y, Liu S, Wang Y, Ren F, Fan X, Liang J, Liu C, Li J, Ju Y, Chang Z, et al. GdX/UBL4A-knockout mice resist collagen-induced arthritis by balancing the population of T h 1/T h 17 and regulatory T cells. *The FASEB J.* 2019;33(7):8375–8385. doi:10.1096/fj.201802217RR.
- Liang J, Li J, Fu Y, Ren F, Xu J, Zhou M, Li P, Feng H, Wang Y. GdX/UBL4A null mice exhibit mild kyphosis and scoliosis accompanied by dysregulation of osteoblastogenesis and chondrogenesis. *Cell Biochem And Function.* 2018;36(3):129–136. doi:10.1002/cbf.3324.
- Li D, Wang L, Shi S, Deng X, Zeng X, Li Y, Li S, Bai P. UBL4A alleviates the progression of intracerebral hemorrhage by regulating oxidative stress and mitochondrial damage. *Exp Anim.* 2024; doi:10.1538/expanim.24-0035.
- Li WX. Computational simulation of JAK/STAT signaling in somatic versus germline stem cells. *Dev Dyn.* 2023;253(7):648–658. doi:10.1002/dvdy.684.
- Hou M, Li H, He T, Hui S, Dai W, Hou X, Zhao J, Zhao J, Wen J, Kan W, et al. Icariside I reduces breast cancer proliferation, apoptosis, invasion, and metastasis probably through inhibiting IL-6/STAT3 signaling pathway. *J Pharm Pharmacol.* 2023;76(5):499–513. doi:10.1093/jpp/rgad103.
- Li Y, Wei J, Sun Y, Zhou W, Ma X, Guo J, Zhang H, Jin T. DLGAP5 regulates the proliferation, migration, invasion, and cell cycle of breast cancer cells via the JAK2/STAT3 signaling Axis. *Int J Mol Sci.* 2023;24(21):24. doi:10.3390/ijms242115819.
- Wang Y, Ning H, Ren F, Zhang Y, Rong Y, Wang Y, Su F, Cai C, Jin Z, Li Z, et al. GdX/UBL4A specifically stabilizes the TC45/STAT3 association and promotes dephosphorylation of STAT3 to repress tumorigenesis. *Mol Cell.* 2014;53(5):752–765. doi:10.1016/j.molcel.2014.01.020.
- Kashyap D, Pal D, Sharma R, Garg VK, Goel N, Koundal D, Zaguia A, Koundal S, Belay A. Global increase in breast cancer incidence: risk factors and preventive measures. *Biomed Res Int.* 2022;2022:1–16. doi:10.1155/2022/9605439.
- Chen H, Li L, Hu J, Zhao Z, Ji L, Cheng C, Zhang G, Zhang T, Li Y, Chen H, et al. UBL4A inhibits autophagy-mediated proliferation and metastasis of pancreatic ductal adenocarcinoma via targeting LAMP1. *J Exp Clin Cancer Res.* 2019;38(1):297. doi:10.1186/s13046-019-1278-9.
- Wang F, Brown EC, Mak G, Zhuang J, Denic V. A chaperone cascade sorts proteins for posttranslational membrane insertion into the endoplasmic reticulum. *Mol Cell.* 2010;40(1):159–171. doi:10.1016/j.molcel.2010.08.038.

27. Bodac A, Mayet A, Rana S, Pascual J, Bowler AD, Roh V, Fournier N, Craciun L, Demetter P, Radtke F, et al. Bcl-xL targeting eliminates ageing tumor-promoting neutrophils and inhibits lung tumor growth. *EMBO Mol Med.* 2023;16(1):158–184. doi:10.1038/s44321-023-00013-x.
28. Vahitha V, Lali G, Prasad S, Karuppiah P, Karunakaran G, AlSalhi MS. Unveiling the therapeutic potential of thymol from *Nigella sativa* L. seed: selective anticancer action against human breast cancer cells (MCF-7) through down-regulation of cyclin D1 and proliferative cell nuclear antigen (PCNA) expressions. *Mol Biol Rep.* 2024;51(1):61. doi:10.1007/s11033-023-09032-w.
29. Liu J, Zhu Y, Wang H, Han C, Wang Y, Tang R. LINC00629, a HOXB4-downregulated long noncoding RNA, inhibits glycolysis and ovarian cancer progression by destabilizing c-myc. *Cancer Sci.* 2024;115(3):804–819. doi:10.1111/cas.16049.
30. Lorusso G, Rüegg C. New insights into the mechanisms of organ-specific breast cancer metastasis. In: *Semi cancer bio.* 2012;22(3):226–233. doi:10.1016/j.semcancer.2012.03.007.
31. Zhang JQ, Li R, Dong XY, He N, Yin RJ, Yang MK, Liu JY, Yu RL, Zhao CY, Jiang T, et al. Design, synthesis and structure-activity relationship studies of meridianin derivatives as novel JAK/STAT3 signaling inhibitors. *Int J Mol Sci.* 2022; 23(4):2199. doi: 10.3390/ijms23042199.
32. Wang W, Renquan Z. Acacetin restrains the malignancy of esophageal squamous carcinoma cells via regulating JAK2/STAT3 pathway. *Chem Biol Drug Des.* 2023;102(3):564–573. doi:10.1111/cbdd.14267.
33. Zhou X, Zhao J, Yan T, Ye D, Wang Y, Zhou B, Liu D, Wang X, Zheng W, Zheng B, et al. ANXA9 facilitates S100A4 and promotes breast cancer progression through modulating STAT3 pathway. *Cell Death Dis.* 2024;15(4):260. doi:10.1038/s41419-024-06643-4.